Water Resources Management (2019) 33:4385–4400
https://doi.org/10.1007/s11269-019-02375-9

Topographic Energy Management in Water Distribution Systems

Roberto del Teso [1] · Elena Gómez [1] · Elvira Estruch-Juan [1] · Enrique Cabrera [1]

Received: 14 March 2019 / Accepted: 4 October 2019 /
Published online: 29 October 2019

Abstract
A significant amount of energy is required to operate pressurised water distribution systems, and therefore, improving their efficiency is crucial. Traditionally, more emphasis has been placed on operational losses (pumping inefficiencies, excess leakage or friction in pipes) than on structural (or topographic) losses, which arise because of the irregular (unchangeable) terrain on which the system is located and the network's layout. Hence, modifying the network to adopt an ecologically friendly layout is the only way to reduce structural losses. With the aim of improving the management of water distribution systems and optimising their energy use, this work audits and classifies water networks' structural losses (derived from topographic energy), which constitutes the main novelty of this paper. Energy can be recovered with PATs (pumps as turbines) or removed through PRVs (pressure reducing valves). The proposed hydraulic analysis clarifies how that energy is used and identifies the most suitable strategy for improving efficiency as locating the most suitable place to install PRVs or PATs. Two examples are discussed to illustrate the relevance of this analysis.

Keywords Topographic energy · Water distribution systems · Energy efficiency · Pressure management · Energy balance

✉ Roberto del Teso
rodete@ita.upv.es

Elena Gómez
elgosel@ita.upv.es

Elvira Estruch-Juan
maesjua1@ita.upv.es

Enrique Cabrera
ecabrera@ita.upv.es

[1] Grupo de Ingeniería y Tecnología del Agua (ITA), Universitat Politècnica de València, Camino de Vera s/n - Edificio 5C, 46022 Valencia, Spain

1 Introduction

Pressure management is unanimously qualified as an essential strategy for improving the efficiency of water networks, as is recognised in the manuals tackling the challenge of reducing water losses from a general perspective (EU 2015). Managing pressure in water networks has been the objective of many papers ranging from general reviews to more specific work dealing with the practicalities of how this ambition can be fulfilled (Walski et al. 2006). Any surplus pressure over the level established in supply standards (urban networks) or over the level required by sprinklers or drip feed systems (irrigation networks) only leads to problems, namely, increased leakage and pipe breakage (Lambert et al. 2013), particularly if the pressure is fluctuating (Agathokleous and Christodoulou 2016). In short, any surplus pressure contributes to water and energy inefficiencies and shortens the average lifespan of pipes (Lambert and Thornton 2012). Moreover, it is worth remembering that managing water pressure has other consequences. On the one hand, citizens who are used to a high pressure associate a low water pressure with a relatively poor service quality. On the other hand, water supply companies report lower earnings in conjunction with lower consumption, which is dependent on the water pressure. In any case, these apparent drawbacks are easily manageable with environmental education.

Since the energy efficiency of a water network is conditioned by its layout, pressure management should begin at the design stage. Dealing with the problem during the design stage (i.e., a top-down approach) and establishing EMAs (energy management areas) (Cabrera et al. 2019), are more effective strategies than modifying an operating system. When a system is already operating, pressure management is implemented as follows:

a) Installing pressure reducing valves (PRVs) to dissipate surplus energy. In addition, by reducing pressure, leaks are minimised, as is the embedded energy, while friction, which is linked to circulating flows, is also reduced (Cabrera et al. 2010). Installing PRVs is the most common method and has been studied in depth concerning its cost, effectiveness and ease of implementation. Different studies have analysed how many PRVs should be installed (Creaco and Franchini 2013), where they should be placed (Saldarriaga and Salcedo 2015) and how to size them (Covelli et al. 2016).
b) Sub-dividing the network into pressure management zones (PMZs) in an attempt to operate them as district metered areas (DMAs) (Lambert et al. 2013). Creating PMZs is highly dependent on the initial network layout (Castro Gama et al. 2014). The differences among EMAs, PMZs and DMAs have been previously discussed (Cabrera et al. 2019).
c) Installing pumps as turbines (PATs). This option maintains the benefits of PRVs (Patelis et al. 2017) and recovers energy, an advantage that compensates for the complexity involved in regulating a hydraulic machine (in which the flow rates are highly variable over time). However, integrating the generated energy into the electricity loop is not a simple matter, and therefore, this approach is usually used for self-consumption. Installing PATs in optimum places obeys criteria similar to those of PRVs (De Paola et al. 2017). This is a mature technology (Fecarotta et al. 2014), although few systems operating at a real scale utilise this option (Muhammetoglu et al. 2017).

In short, we can “reduce”, “recover” or “remove” surplus energy linked to excess pressure (Cabrera et al. 2019). The differences among these strategies are significant. Reducing focuses on pressure (an intensive variable), whereas recovering and removing refer to energy (an

extensive variable). Therefore, by modifying the layout, both pressure and structural losses (Cabrera et al. 2019) are reduced at the source. By installing PRVs or PATs, the initial balance is altered with a new energy term, equal to the flow through them times the decrease in pressure they produce.

This paper reviews energy concepts that have already been introduced concerning water distribution systems, particularly the differences between operational and structural losses. This review also updates the terminology related to the energy balance employed in previous papers. Structural losses, the subject of this paper, are then broken down to assess and manage topographic energy with the aim of improving water transport efficiency. The focus of this proposed comprehensive approach is illustrated in two networks (branched and looped).

Finally, the differences between the traditional approaches and the method suggested in this paper are highlighted. Most of the current methodologies consist of optimisation algorithms (that is, mathematical tools) that seek to minimise pressures and leaks (Creaco and Pezzinga 2018). Our focus straightforwardly aims to minimise structural energy losses. Although structural energy losses are strongly related to pressure and leaks, they are different concepts. Therefore, the proposed method is mainly a physics approach, which can be easily followed in the simple proposed examples. In any case, guidelines to generalise the procedure to complex real systems are duly outlined.

2 Pressurized Water Transport Systems: Basic Energy Concepts

The aim of a pressurised water distribution system is to efficiently deliver the water flow users require (Q) at the established pressure (p). The result (Q·p) is related to the power required by users, which, extended over a specific period of time, is the energy delivered to users. If water is supplied at the pressure established in the standards, the sum of the energy delivered to each user (j) is the minimum energy required by the system E_{uo}:

$$E_{uo} = \gamma \sum_{j=1}^{n} v_{c,j} \left[\left(z_j - z_l \right) + \frac{p_{0,j}}{\gamma} \right] \tag{1}$$

where γ is the specific weight of water; n is the number of users; j is the index for users, ranging from 1 to n; $v_{c,j}$ is the volume of water consumed at node j during the considered period; z_j the height of node j; and $\frac{p_{0,j}}{\gamma}$ is the minimum supply pressure at node j. The height of the lowest node in the system, z_l, is the reference system height.

The total energy supplied to the system, E_{sr}, is calculated by adding E_{uo} to the energy losses in the system (operational and structural losses). These concepts, in addition to those that will be discussed in this work, have been established in previous works (Cabrera et al. 2010, 2015, 2019).

2.1 Energy Supply Sources

Water supply sources inject water into the system, adding a specific amount of energy per unit volume (kWh/m^3), thereby conditioning the energy efficiency of the network. If the established pressure is exceeded at the least favourable node, this leads to system inefficiency.

Depending on whether supply sources are able to regulate the hydraulic head, those sources can be either rigid or variable (Cabrera et al. 2019). Tanks and reservoirs supply gravitational

energy to water, and since the height of the supply, H_{hi}, is almost constant (with only small level variations inside the tanks), the hydraulic head cannot be regulated. Tanks and reservoirs are therefore rigid sources. On the other hand, pumps installed with variable-frequency drivers are variable energy sources because the unitary injected energy, H_{hi}, can be adjusted by modifying their operating point.

2.2 Operational Losses

Operational losses are those that depend on the operation of the network. These losses are located in pumping stations, E_{pr}, in pipes as a result of friction, E_{fr}, and through leaks, E_{lr}. There are other losses, such as breakages in tanks, in the network itself or in household tanks, all of which are collectively denoted as E_{or}.

The first source of losses, E_{pr}, is the one that usually requires closer attention. These losses are obtained directly from different pump characteristic curves. In this work, E_{pr} is not considered. The second source of losses in the network, that is, friction losses, E_{fr}, is expressed in Eq. 2 for a given time interval, Δt (Cabrera et al. 2010):

$$E_{fr} = \gamma \sum_{i=1}^{m} q_i \Delta h_i \Delta t = \gamma \sum_{i=1}^{m} v_i \Delta h_i \tag{2}$$

where q_i is the flow in pipe i; m is the number of pipes; Δh_i is the head loss in pipe i; and v_i is the volume through pipe i in the given time interval. Nevertheless, as the energy balance is nodal, it is worth expressing friction losses in terms of nodes, leading to the following:

$$E_{fr} = \gamma \sum_{j=1}^{n} v_{g,j} \left[H_{hi} - \left((z_j - z_l) + \frac{p_j}{\gamma} \right) \right] \tag{3}$$

where $v_{g,j}$ is the total volume at node j, equal to the water demand at node $v_{c,j}$ plus the leaked volume $v_{l,j}$ through half of the pipes converging at node ($v_{g,j} = v_{c,j} + v_{l,j}$), while $\frac{p_j}{\gamma}$ is the pressure at node j. Equation 3 therefore provides the friction losses occurring between the source and each node for the total volume of water in each of the nodes. Analytically, Eqs. 2 and 3 give the same result. Removing the consumed volume at the corresponding node from Eq. 3, the nodal formulation allows a direct calculation of the total contribution of leaks to friction losses.

In systems with multiple sources, the percentage of water that arrives at each node from any of the sources must be known. In this case, the nodal friction E_{fr} should be calculated by weighting, according to each source, the friction corresponding to the water volume at each node, as stated in Eq. 4:

$$E_{fr} = \gamma \sum_{j=1}^{n} \sum_{s=1}^{k} \alpha_{s,j} \, v_{g,j} \left[H_{hi,s} - \left((z_j - z_l) + \frac{p_j}{\gamma} \right) \right] \tag{4}$$

where $\alpha_{s,j}$ is the percentage of water arriving at node j coming from source s; $H_{hi,s}$ is the piezometric head of the corresponding source s; and k is the number of sources. In what follows, we assume systems with only one source.

On the other hand, the embedded energy in leaks (E_{lr}) is equal to the leaked volume by the piezometric height at the node where the leak is located. This leads to the following nodal equation:

$$E_{lr} = \gamma \sum_{j=1}^{n} v_{l,j} \left[\left(z_j - z_l\right) + \frac{p_j}{\gamma} \right] \tag{5}$$

Finally, if the supply is coming from a variable source and there is an excess pressure at the critical node, this is attributed to a deficient pumping regulation, as the energy requirements have not been adjusted to the critical node needs. This energy surplus, E_{er}, is therefore an operational loss, as shown in Fig. 1a. The value for this loss is obtained as follows:

$$E_{er} = \gamma \sum_{j=1}^{n} v_{g,j} \left(\frac{p_{min}}{\gamma} - \frac{p_{0,j}}{\gamma} \right) \tag{6}$$

where $\frac{p_{min}}{\gamma}$ is the minimum pressure in the system. If the energy source is a rigid source, the excess pressure at the critical node is a structural loss, which is explained as follows.

2.3 Structural Losses: Topographic Energy

While operational losses depend on how the system is managed, structural losses are inherent to the topography and layout (network, tank heights, etc.). Since users are located at different heights, to supply the right pressure to the critical node, the remaining nodes are supplied at a pressure over the required minimum. Consequently, more energy will be delivered than is required. Topographic energy (E_{tr}) is basically excess energy linked to the topography and network structure, as its name suggests (Cabrera et al. 2015). Topographic energy is not in itself a loss of energy, as is the case of energy lost through operational losses. However, topographic energy is still an inefficiency and should be corrected as far as is reasonably possible since it means that more energy is supplied than is strictly necessary. The value of topographic energy is obtained as follows:

$$E_{tr} = \gamma \sum_{j=1}^{n} v_{g,j} \left(\frac{p_j}{\gamma} - \frac{p_{0,j}}{\gamma} \right) - E_{er,j} \tag{7}$$

The excess energy existing in each node, $E_{er,j}$, must be subtracted to avoid quantifying it as topographic energy. Tanks (as with any rigid energy source) lead to inefficiencies since they are unable to adapt to the exact energy requirements at the critical node over time. In the best-case scenario, with the height being designed to avoid excesses at the least favourable node during peak hours, as demand falls, there will be an energy excess (inefficiency) at the critical

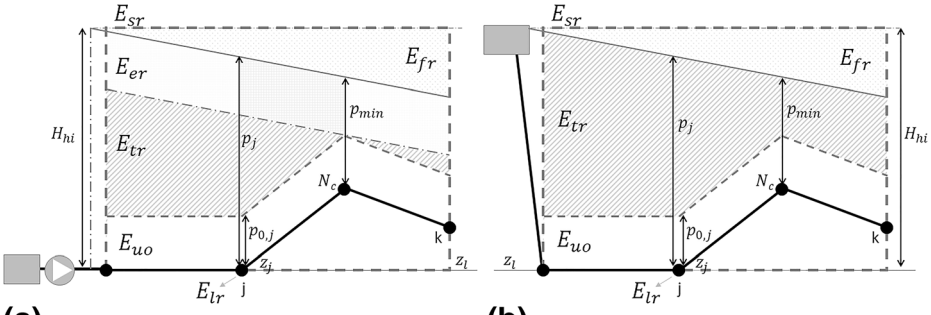

Fig. 1 Graphic illustrations of the energy balance for **a** variable and **b** rigid energy sources

point. While pumps can be regulated, tanks cannot (they have small level variations that are not used to regulate the pressure within the system). Consequently, energy surpluses are considered inevitable. Figure 1 illustrates the difference (Fig. 1a shows the situation for a variable source, while Fig. 1b shows that for a rigid source).

Finally, it must be stated that operational and structural losses are coupled. The former depend on the hydraulic gradient (variable over time), which in turn conditions the latter. Therefore, overall optimisation requires a comprehensive analysis.

3 Topographic Energy Breakdown

To reduce topographic energy as far as possible without compromising the supply pressure at nodes, topographic energy should be broken down into three categories: unavoidable (E_{tr}^{u}), linked to flow (E_{tr}^{f}) and manageable (E_{tr}^{m}), as displayed in Fig. 2. To calculate these components, the downstream path (or paths) of the flow from the analysis node (start point) must be known. This is necessary to guarantee the required supply pressure at all nodes. Hence, a comprehensive analysis of the system is carried out, thus avoiding correction factors (Giugni et al. 2014). The process is described in the following.

3.1 Unavoidable Topographic Energy

Unavoidable topographic energy is linked to the energy needed to supply a high-elevation point in a network in an ideal situation (no friction losses). Such energy cannot be avoided except by modifying the layout and can be defined as follows:

$$E_{tr}^{u} = \gamma \sum_{j=j}^{k} v_{g,j}\left(z_{h,j\to k} - z_j\right) \tag{8}$$

where $z_{h,j\to k}$ is the height of the highest node along the possible paths between the study node j and nodes k. The k nodes are the final points of consumption along the paths carrying water downstream from j. In branched networks, the k nodes are always terminal nodes, and there will be as many paths as there are end nodes. Figure 3a shows that to analyse node N1 (study

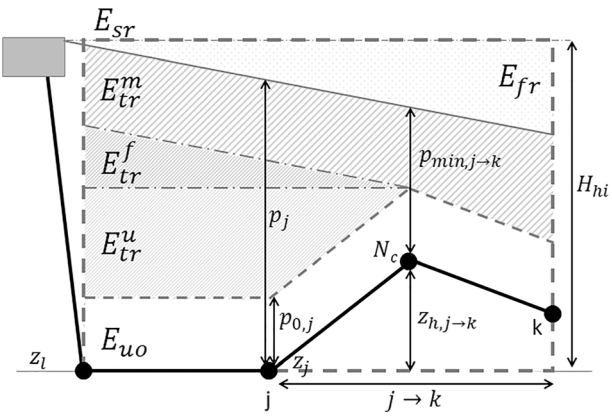

Fig. 2 Topographic energy breakdown with a rigid supply source

node j), there are two paths of water downstream from N1 that end at nodes N2 and N3 (the k nodes). In looped networks, the situation is similar, but we need to bear in mind that water can flow down different paths from j to the same k node, and consequently, all of them must be analysed. To analyse node N1 in Fig. 3b, there are two different paths leading to the same k node, i.e., node N3. Among all the nodes along the paths flowing between j and k, the height of the highest node of all will be $z_{h,\,j\to k}$.

Water paths are obtained following the direction of circulation of the water flow. In branched networks, water always flows in the same direction, and its determination can be simply performed: the flow has only to be followed from the source through the system, and the different paths that appear at bifurcations need to be determined. In looped networks, any change, such as the demand pattern during the day, can impact the water flow direction. This is not difficult with calculus, as paths are determined at each instant of time. For this purpose, the water flow is again followed from the source until it reaches a node where there is a junction of pipes. Any of the pipes in the node creates a new path. Each path ends when it arrives at a node that is already part of the path or when it arrives at a node without any outgoing flow (see node N3 in Fig. 3b). This process of determining paths can be automated once the sense of the water flow is known in each pipe. It requires a hydraulic simulation software package that provides the sense of the water flow.

The unavoidable topographic energy (E_{tr}^{u}) is therefore conditioned by the highest points in the network. At all nodes upstream from the highest point that are located at required heights lower than or equal to this highest point, a part of the topographic energy is unavoidable. Figure 2 shows how node j has a lower required height than node Nc; therefore, this part of the topographic energy is unavoidable since the flow has to overcome this difference. Unavoidable topographic energy therefore depends on the height differences within the network and the network design.

3.2 Unavoidable Flow-Dependent Topographic Energy

This component of the topographic energy is necessary to meet the minimum pressure required at the nodes. Reducing it would mean that the required supply pressure would not be reached

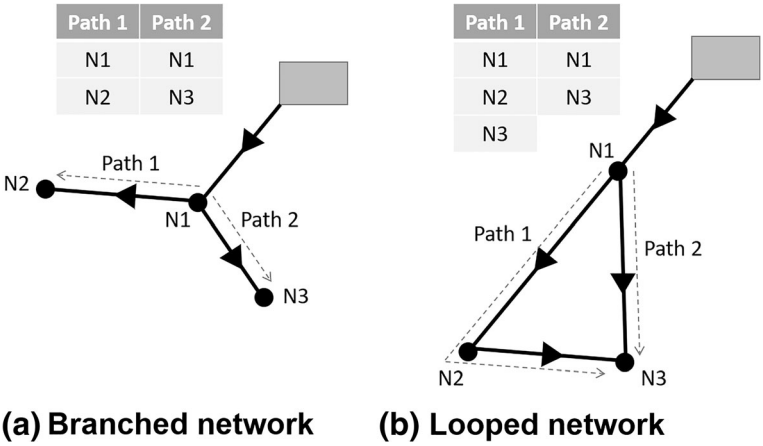

Fig. 3 Possible paths between the study node j and nodes k for **a** a branched network and **b** a looped network

at nodes located downstream. This depends on the hydraulic gradient of the system, and consequently, flow-dependent topographic energy, E_{tr}^{f}, is considered:

$$E_{tr}^{f} = \gamma \sum_{j=j}^{k} v_{g,j}\left(z_j + \frac{p_j}{\gamma} - \frac{p_{min,j\to k}}{\gamma} - z_{h,j\to k}\right) \tag{9}$$

where $p_{min,\,j\to k}$ is the least favourable node pressure from among the possible paths of flow between study node j and all end nodes k. To assess the minimum pressure between j and k, the midway nodes without demand are not relevant.

3.3 Manageable Topographic Energy and Accumulated Topographic Energy

The dispensable part of topographic energy is defined as manageable and is equal to:

$$E_{tr}^{m} = \gamma \sum_{j=j}^{k} v_{g,j}\left(\frac{p_{min,j\to k}}{\gamma} - \frac{p_{0,j}}{\gamma}\right) - E_{er,j} \tag{10}$$

Manageable topographic energy can be recovered (using PATs) or dissipated (using PRVs). Figure 4b shows that a PRV introduces a height reduction equal to the dissipated manageable topographic energy to the line of piezometric heights. This manageable topographic energy becomes dissipated energy through friction in the PRV.

Finally, to identify the ideal point at which to install a PRV, the concept of accumulated topographic energy is defined as the total manageable topographic energy pertaining to the path that begins at node j and ends at node k, leading to:

$$\Delta E_{tr,j}^{m} = \gamma \left(\sum_{j=j}^{k} v_{g,j}\right)\left(\frac{p_{min,j\to k}}{\gamma} - \frac{p_{0,j}}{\gamma}\right) - \sum_{j=j}^{k} E_{er,j} \tag{11}$$

The sum includes the total volume $v_{g,j}$ of the nodes along the flow path between study node j and end node k, taking into account that a node can be on more than one path (Fig. 3). In short, the total volume of all nodes downstream from start node j must be considered, as must the fact that all nodes are on one of the possible paths leading to node k. Similarly, we need to consider the sum of the surplus energy between nodes j and k, where applicable.

The ideal point at which to install a PRV or PAT is the location where the highest amount of manageable topographic energy is accumulated. This node is able to dissipate (or recover) the

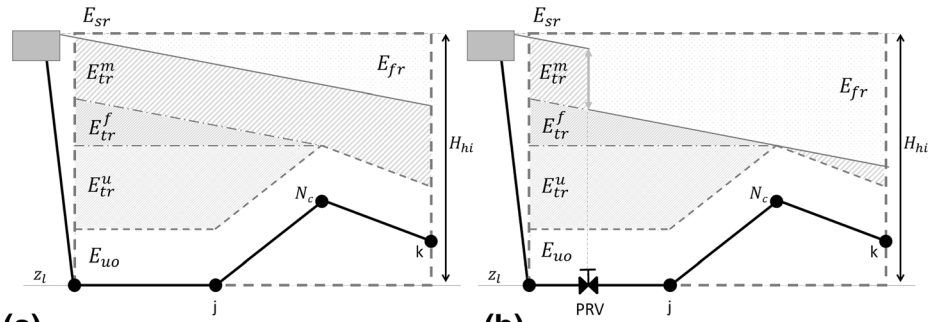

Fig. 4 Managing topographic energy without a PRV (**a**) and with a PRV (**b**)

maximum amount of topographic energy. After the first device (PAT or PRV) has been installed, a new study is required to identify where the next device should be installed.

The topographic energy, E_{tr}, can be expressed as:

$$E_{tr} = E_{tr}^{u} + E_{tr}^{f} + E_{tr}^{m} \tag{12}$$

To specify the magnitude and type of topographic energy in the system, two indicators are defined, namely, θ_t and θ_{tm}. The first indicator, θ_t, represents the percentage of topographic energy E_{tr} within the total energy supplied to the system E_{sr}:

$$\theta_t = \frac{E_{tr}}{E_{sr}} \tag{13}$$

If the terrain is very irregular or if tanks are located higher than necessary, this value will be high (θ_t will nearly equal 1), as topographic energy will represent a high percentage of the total energy supplied. In flat networks with energy efficient layouts, θ_t will be closer to 0. Nevertheless, this information is incomplete since it says nothing about whether the topographic energy is manageable. This information is provided by another indicator, θ_{tm}:

$$\theta_{tm} = \frac{E_{tr}^{m}}{E_{tr}} \tag{14}$$

This indicator represents the percentage of manageable topographic energy over the total topographic energy. These two indicators provide relevant (and complementary) information about the system.

It is worth analysing the relationship between topographic energy (and its components) and the features of the system:

a) Influence of the network layout: In systems with supply points located at different heights, topographic energy can be important. Changes in the layout can reduce topographic energy (Cabrera et al. 2019).
b) Influence of the energy source: With a rigid supply source, part of the topographic energy can be managed. With a variable source of energy, if it exists excess energy, it can be avoided by regulating the pumping station.
c) Influence of the system profile: Depending on the profile of the network, topographic energy will be either manageable or unavoidable.

4 Breakdown of Structural Losses Linked to Leaks

After having characterised structural losses, we need to discuss some relative aspects of the energy balance. Losses embedded in leaks, E_{lr} (Eq. 5), are operational losses that are dependent primarily on the water pressure. This term is broken down into two summands. The first includes leaks at standard pressure (E_{lr}^{o}), whereas the second addresses leaks when there is an excess pressure $\left(E_{lr}^{te}\right)$, leading to:

$$E_{lr} = \gamma \sum_{j=1}^{n} v_{l,j}\left[\left(z_j - z_l\right) + \frac{p_j}{\gamma}\right] == \gamma \sum_{j=1}^{n} v_{l,j}\left[\left(z_j - z_l\right) + \frac{p_{o,j}}{\gamma}\right] + \gamma \sum_{j=1}^{n} v_{l,j}\left(\frac{p_j - p_{0,j}}{\gamma}\right) = E_{lr}^{o} + E_{lr}^{te} \tag{15}$$

Consequently, the operational loss linked to leaks is E_{lr}^{o}, whereas the complementary summand E_{lr}^{te} is included in the topographic energy and excess energy. This approach means we are able to calculate the amount of energy embedded in leaks caused by topographic energy and excess energy. This leads to the following energy balance:

$$E_{sr} = \gamma \left(\sum_{j=1}^{n} v_{g,j} \right) H_{hi} = E_{uo} + E_{pr} + E_{fr} + E_{lr}^{o} + E_{er} + E_{tr} \tag{16}$$

Operational losses through pumping E_{pr} and excess energy E_{er} are zero in the case of systems supplied through rigid sources. This balance does not include other types of losses (E_{or}), such as load breakages in tanks.

Installing PRVs modifies the values of these terms. The energy dissipated by PRVs is integrated into E_{fr}, whereas E_{tr} will decrease by the same amount. If a PAT is installed, on the one hand, operational losses (those of the hydraulic machine) will be included in E_{fr}; on the other hand, the energy the turbine produces must be subtracted from E_{sr}, whereas E_{tr} will diminish (energy withdrawn by the PAT).

5 Methodology Application and Generalisation

The preceding analyses require the flow directions to be known. The minimum pressure required at a node without compromising nodes further downstream can only be determined if the flow direction is known. Therefore, knowing the water path is fundamental. In branched networks, the flow path is immediately formed and does not vary. In looped networks, the paths may depend on the load status of the network. Nevertheless, PRVs and PATs can only be installed in pipes with only one flow direction; therefore, this flow direction must be properly defined. To focus on the discussed concepts, the two example networks are static. In dynamic networks, an analysis is performed for each network status, after which the set of energies is superimposed, and all the results are integrated for the final analysis.

The authors have developed an algorithm to determinate the water paths in both branched and looped networks that allows complex structural energy audits to be performed. As the focus of this paper is on the new concepts and the proposed procedure, the cases presented are simple to allow the methodology to be better understood.

5.1 Case Study 1: Branched Network

A variable supply source injects water into the branched network of Fig. 5. This figure also includes the pipes' diameters and lengths (with a roughness if 0.1 mm) and different flow paths in the network. There are 6 possible paths through which water can flow, as in branched networks, the number of paths is equal to the number of end nodes. The pump is located at the lowest height ($z_1 = 0$ m) and supplies the flow at a pressure of 78.54 mWc ($H_{hi} = 78.54$ m). No losses at the pumping station are deemed to exist. The reference pressure is 15 m at all consumption nodes ($\frac{p_0}{\gamma} = 15$ mWc). Hydraulic calculations are carried out using EPANET; therefore, the results are obtained assuming a demand-driven approach for user consumption, while leaks (loaded as emitters) are considered pressure-driven demand. Nevertheless, this nodal structural loss audit could be improved with a global pressure-driven formulation (Ciaponi and Creaco 2018). The proposed structural losses audit could be performed from

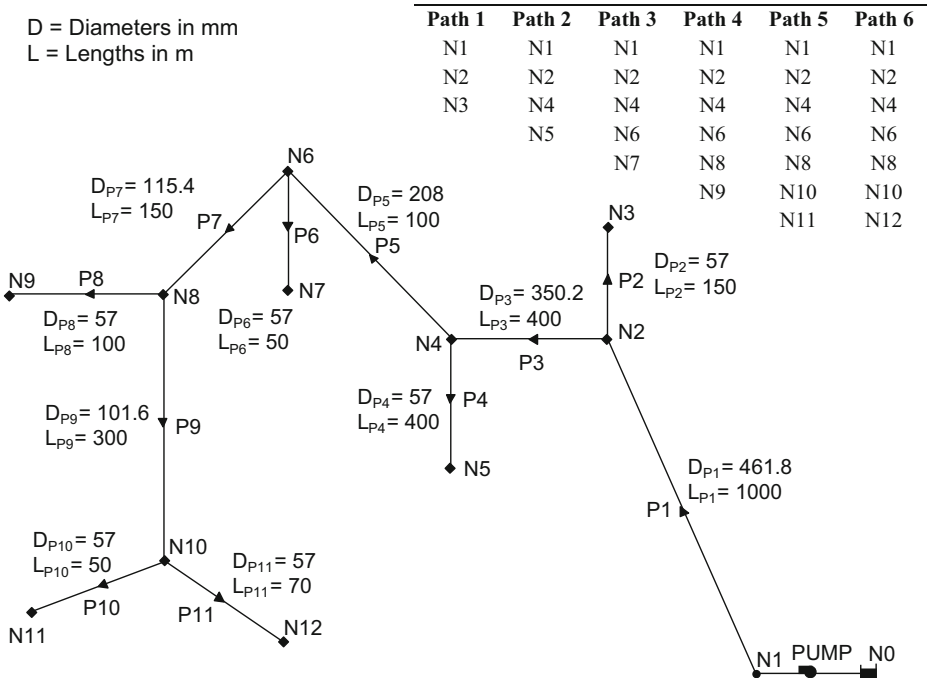

Fig. 5 Branched network with a variable supply source

any of these two perspectives. Nevertheless, regardless of the approach followed, both the concepts explained and the methodology followed would not change.

The node data (height, total demand, consumption and leaks) are shown in the first four columns of Table 1. The final three columns in Table 1 show the following: p_j, the pressure at each node; $z_{h,\,j\rightarrow k}$, the greatest height of the set of nodes, including study node j, which are downstream from study node j on any of the possible paths; and $p_{min,\,j\rightarrow k}$, the minimum pressure resulting from applying identical criteria. Having established the paths, the least favourable node in the network is identified as the one with the least pressure. In this case, the

Table 1 Node features in the branched network

Node ID	z_j (m)	$v_{g,\,j}$ (l/s)	$v_{c,\,j}$ (l/s)	$v_{l,\,j}$ (l/s)	p_j (mWc)	$z_{h,\,j\rightarrow k}$ (m)	$p_{min,\,j\rightarrow k}$ (mWc)
N3	50	3.97	3.83	0.14	20.34	50	20.34
N2	40	2.98	2.78	0.20	38.44	55	20.34
N4	40	0.20	0	0.20	38.33	55	20.82
N5	25	4.20	4.03	0.17	29.26	25	29.26
N6	55	1.65	1.5	0.15	23.06	55	20.82
N7	45	4.56	4.39	0.17	29.54	45	29.54
N8	45	2.95	2.78	0.17	28.37	45	20.82
N9	45	4.73	4.58	0.15	20.82	45	20.82
N10	15	3.01	2.78	0.23	51.56	15	51.56
N11	10	4.23	4	0.23	53.51	10	53.51
N12	5	4.49	4.25	0.24	56.77	5	56.77
N1	0	0.00	0	0.00	78.54	55	20.34
N0	0	–	–	–	–	–	–

Table 2 Energy obtained (nodal and overall) in the network (kWh/h)

Nodes	E_{uo}	E_{fr}	E^{o}_{lr}	E^{te}_{lr}	E_{er}	E_{tr}	$E^{u}_{tr,j}$	$E^{f}_{tr,j}$	$E^{m}_{tr,j}$	$\Delta E^{m}_{tr,j}$	E_{sr}
N3	2.44	0.32	0.09	0.01	0.21	0.00	0.00	0.00	0.00	0.00	3.06
N2	1.50	0.00	0.11	0.05	0.15	0.54	0.44	0.09	0.01	0.10	2.29
N4	0.00	0.00	0.11	0.05	0.00	0.05	0.03	0.00	0.01	0.23	0.15
N5	1.58	1.00	0.07	0.02	0.21	0.38	0.00	0.00	0.38	0.38	3.24
N6	1.03	0.01	0.11	0.01	0.08	0.05	0.00	0.04	0.02	0.19	1.27
N7	2.58	0.18	0.10	0.02	0.23	0.42	0.00	0.00	0.42	0.42	3.52
N8	1.64	0.15	0.10	0.02	0.15	0.24	0.00	0.22	0.02	0.15	2.27
N9	2.70	0.59	0.09	0.01	0.24	0.03	0.00	0.00	0.03	0.03	3.64
N10	0.82	0.35	0.07	0.08	0.15	0.93	0.00	0.00	0.93	3.63	2.32
N11	0.98	0.62	0.06	0.09	0.21	1.39	0.00	0.00	1.39	1.39	3.26
N12	0.83	0.74	0.05	0.10	0.22	1.62	0.00	0.00	1.62	1.62	3.46
Total	16.10	3.96	0.96	0.46	1.85	5.65	0.47	0.35	4.83	–	28.5

least favourable node is N3 (with a minimum pressure of 20.34 mWc), which, as can be seen, is not the highest node.

Table 2 shows the different overall energy balance terms by node (pumping losses are not considered) and characterises the system's topographic energy. This table includes the term E^{te}_{lr} (already counted in E_{tr}), a fact that must be taken into account when establishing the sum provided by the overall balance E_{sr}.

The balance includes excess energy because the minimum pressure, 20.34 mWc, exceeds the required amount, 15 mWc (variable supply source). The difference between these two values is modest because the excess is not significant.

Two actions can be taken to improv the system's efficiency: adjusting the minimum pressure to the established supply requirements (reducing the speed of the pump) and installing a PRV. Table 2 shows where the PRV should be installed, namely, at N10, where more manageable topographic energy is accumulated than at any other node. Table 3 compares the initial and final scenarios after implementing these two improvements. The values are rather modest because of the analysed energy period. An annual calculation must be multiplied by the hours per year the system is operated.

The following conclusions are drawn from this comparison:

- By reducing the relative speed of the pump to 0.976, the pressure at the critical node equals the required pressure. This is more efficient than installing a PRV since, with this action, the E_{er} term is eliminated, reducing the E_{sr} term (ΔE_{sr}=2.3 kWh/h).
- The contribution of the PRV to energy efficiency is marginal. The reduction in manageable topographic energy (3.70 kWh/h) is compensated by the increase in friction within the PRV (ΔE_{fr}=3.40 kWh/h). The difference between these variations (0.30 kWh/h) is mainly

Table 3 Total energy (kWh/h) in the branched network

	E_{uo}	E_{fr}	E^{o}_{lr}	E^{te}_{lr}	E_{er}	E_{tr}	E^{u}_{tr}	E^{f}_{tr}	E^{m}_{tr}	E_{sr}	θ_t	θ_{tm}
Initial scenario	16.10	3.96	0.96	0.46	1.85	5.65	0.47	0.35	4.83	28.5	0.20	0.86
Final scenario	16.10	7.36	0.78	0.12	0	1.96	0.46	0.37	1.13	26.2	0.07	0.58

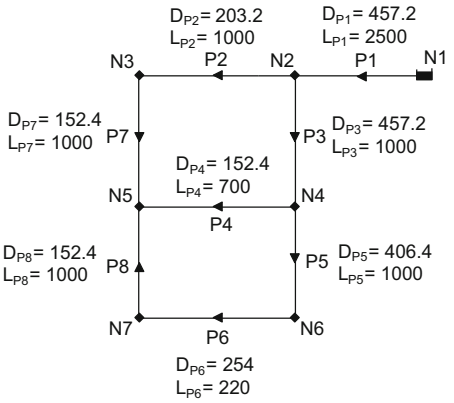

Path 1	Path 2	Path 3
N1	N1	N1
N2	N2	N2
N3	N4	N4
N5	N5	N6
		N7
		N5

D = Diameters in mm
L = Lengths in m

Fig. 6 Looped network and flow paths

due to the energy reduction linked to leaks, as a reduction in flow rates impacts on lower friction losses.

- Table 2, particularly column $\Delta E^{m}_{tr,j}$, pinpoints the optimum location of the PRV to be installed, in this case, at N10. A second analysis with the PRV installed allows us to identify the optimum point at which to install a second PRV (N7).
- Once the PRV has been installed, the indicators referring to topographic energy improve.

On the basis of the information provided in Table 3, each contribution can be studied individually while passing through intermediate stages (i.e., the pump adjustment without and with a PRV).

5.2 Case Study 2: Looped Network

The second example is the looped network depicted in Fig. 6, supplied from a rigid source (N1). The operating pressure is 30 mWc. Table 4 (similar to Table 1) shows the nodes specifications (with a roughness of 0.1 mm) of this network. The arrows show the path of the flow, which is invariable in this load status. The height of the lowest node (N2) is taken as the reference (z_f=50 m).

N5 is the end of all three possible paths regardless of the path chosen (Fig. 6).

Table 5 shows the nodal and total energy balances (kWh/h), included the topographic energy breakdown. The maximum accumulated topographic value is at node N6, and thus, the

Table 4 Node features in the looped network

Node ID	z_j (m)	$v_{g,j}$ (l/s)	$v_{c,j}$ (l/s)	$v_{l,j}$ (l/s)	p_j (mWc)	$z_{h,j\to k}$ (m)	$p_{min,j\to k}$ (mWc)
N2	50	25.84	25	0.84	142.8	150	37.9
N3	150	30.43	30	0.43	37.92	150	37.9
N4	120	30.59	30	0.59	71.25	120	71.3
N5	90	23.69	23	0.69	97.75	90	97.8
N6	80	40.73	40	0.73	109.84	90	97.8
N7	80	60.73	60	0.73	108.51	90	97.8
N1	200	0.00	0	0.00	0.0	200	37.9

Table 5 Nodal and total energy balances (kWh/h)

Nodes	E_{uo}	E_{fr}	E^{o}_{lr}	E^{te}_{lr}	E_{er}	E_{tr}	$E^{u}_{tr,j}$	$E^{f}_{tr,j}$	$E^{m}_{tr,j}$	$\Delta E^{m}_{tr,j}$	E_{sr}
N2	7.36	14.50	0.25	0.93	0.00	28.59	25.35	1.24	2.01	16.47	50.70
N3	38.26	18.53	0.55	0.03	0.00	2.36	0.00	0.00	2.36	4.20	59.72
N4	29.43	17.63	0.58	0.24	0.00	12.38	0.00	0.00	12.38	63.02	60.02
N5	15.79	14.47	0.47	0.46	0.00	15.77	0.00	0.00	15.75	15.75	46.48
N6	23.54	24.04	0.43	0.57	0.00	31.90	4.00	0.84	27.07	83.18	79.91
N7	35.32	36.63	0.43	0.56	0.00	46.77	5.96	0.45	40.36	56.11	119.15
Total	149.70	125.80	2.71	2.79	0.00	137.77	35.31	2.53	99.93	–	415.98

PRV should be installed just upstream of N6 and set at 55 mWc, thereby guaranteeing 30 mWc at all nodes (N3 is the critical node).

Similar to Table 3, Table 6 compares the energy audits without and with a PRV. The main difference lies in the fact that with the PRV installed, the water flow in line P8 changes its direction, and the new end of the line becomes N7. After the PRV is installed, $\theta_t = 0.19$. If further energy reduction is required, a second PRV can be installed. Any additional analysis should consider the three new paths ending at N7.

As in the preceding example (the branched network), the PRV barely contributes to improving the energy efficiency of the network since the reduction in manageable topographic energy (62.03 kWh/h) is counteracted by a friction increase (60 kWh/h). In this case, as there are fewer leaks in the looped network than in the branched network, the differences are even lower.

6 Conclusions

The global energy analysis performed in this study from a strictly hydraulic perspective allows topographic energy to be better managed. This energy, although necessary, is inefficient because of the excess pressure over and above the reference value. These losses, called structural losses, should be reduced beginning at the design stage (through an ecologically friendly layout); when a system is already operating, the possibilities to manage these losses are limited. Recovering or removing part of the existing topographic energy are available options. To better understand and assess the improvement possibilities, it is worth breaking topographic energy down into unavoidable, unavoidable flow-dependent and manageable components. Only the third component can be recovered (using PATs) or removed (using PRVs).

From the energy audit of structural losses, the main novelty of this paper, that is, a strategy that should be followed to break down topographic energy based on a nodal energy analysis, is presented. The proposed methodology analyses the energy at each node and performs a downstream comparison through to the end node on the path. The ultimate aim is to calculate

Table 6 Total hourly energy (kWh/h) of the looped network with and without a PRV

	E_{uo}	E_{fr}	E^{o}_{lr}	E^{te}_{lr}	E_{er}	E_{tr}	E^{u}_{tr}	E^{f}_{tr}	E^{m}_{tr}	E_{sr}	θ_t	θ_{tm}
Without a PRV	149.7	125.8	2.71	2.79	0	137.77	35.31	2.53	99.93	415.98	0.33	0.73
With a PRV	149.7	185.8	2.35	1.72	0	77.08	25.35	13.82	37.90	414.90	0.19	0.49

the accumulated topographic energy at each node for each load status. The final sum (superimposing all load statuses) indicates all the energy efficiency benefits of installing a PRV (or PAT), including the benefits stemming from reducing leaks. This automated process, based on a hydraulic model, is capable of analysing real networks.

In summary, while the focus of traditional approaches is on minimising leaks and pressures using mathematical optimisation techniques, this new methodology seeks to maximise the system's energy efficiency through a hydraulic procedure. Consequently, final decisions can be made with a clearer view of the system's behaviour.

Acknowledgments The authors acknowledge the very careful review made by the three anonymous reviewers which, indeed, improved the understandability and quality of this paper.

Compliance with Ethical Standards

Conflict of Interest None.

Glossary

$\Delta E^{m}_{tr,j}$	Accumulated manageable topographic energy at node j
$\alpha_{s,j}$	percentage of water arriving at the node j that comes from source s
γ	water specific weight
θ_t	percentage of total topographic energy = E_{tr}/E_{sr}
θ_{tm}	percentage of manageable topographic energy; real case = $\frac{E^{m}_{tr}}{E_{tr.}}$
E_{er}	Energy supplied in excess for the real systems
E^{f}_{tr}	flow topographic energy
E_{fr}	Energy dissipated through friction in pipes and valves
E_{lr}	Energy embedded in leaks;
E^{m}_{tr}	Manageable topographic energy
E_{or}	Other energy operational losses
E_{pr}	Energy pumping station losses;
E_{sr}	total supplied energy for the real systems
E^{te}_{lr}	Energy embedded in leaks caused by overpressure
E_{tr}	topographic energy required by the real system
E^{u}_{tr}	Unavoidable topographic energy
E_{uo}	minimum required energy by users
H_{hi}	highest piezometric head
$H_{hi,s}$	piezometric head of the corresponding source s
$p_{0,j}/\gamma$	required pressure (established by standards) at the generic node j
p_j/γ	pressure at the generic node j
p_{min}/γ	minimum pressure
$p_{min,j\to k}/\gamma$	minimum pressure between nodes j and k
$v_{c,j}$	volume demand at node j
$v_{l,j}$	volume leakage at node j
$v_{g,j}$	total volume at node j = $v_{c,j} + v_{l,j}$.
$z_{h,j\to k}$	highest node elevation between nodes j and k
z_j	Elevation of node j
z_l	lowest node elevation

References

Agathokleous A, Christodoulou S (2016) Vulnerability of urban water distribution networks under intermittent water supply operations. Water Resour Manag 30:4731–4750. https://doi.org/10.1007/s11269-016-1450-3

Cabrera E, Pardo MA, Cobacho R, Cabrera E (2010) Energy audit of water networks. J Water Resour Plan Manag 136(6):669–677. https://doi.org/10.1061/(ASCE)WR.1943-5452.0000077

Cabrera E, Gómez E, Cabrera E, Soriano J, Espert V (2015) Energy assessment of pressurized water systems. J Water Resour Plan Manag 141(8):04014095. https://doi.org/10.1061/(ASCE)WR.1943-5452.0000494

Cabrera E, Gómez E, Soriano J, del Teso R (2019) Towards eco-layouts in water distribution systems. J Water Resour Plan Manag 145(1):04018088. https://doi.org/10.1061/(ASCE)WR.1943-5452.0001024

Castro Gama ME, Quan P, Andreja J, Chiesa C (2014) Model-based Sectorization of water distribution networks for increased energy efficiency. 11th International Conference on Hydroinformatics. HIC 2014, New York City, USA

Ciaponi C, Creaco E (2018) Comparison of pressure-driven formulations for WDN simulation. Water 10(4):523. https://doi.org/10.3390/w10040523

Covelli C, Cozzolino L, Cimorelli L, Della Morte R, Pianese D (2016) Optimal location and setting of PRVs in WDS for leakage minimization. Water Resour Manag 30(5):1803–1817. https://doi.org/10.1007/s11269-016-1252-7

Creaco E, Franchini M (2013) A new algorithm for real-time pressure control in water distribution networks. Water Supply 13(4):875–882. https://doi.org/10.2166/ws.2013.074

Creaco E, Pezzinga G (2018) Comparison of algorithms for the optimal location of control valves for leakage reduction in WDNs. Water 10(4):466. https://doi.org/10.3390/w10040466

De Paola F, Giugni M, Portolano D (2017) Pressure management through optimal location and setting of valves in water distribution networks using a music-inspired approach. Water Resour Manag 31:1517. https://doi.org/10.1007/s11269-017-1592-y

EU (European Union) (2015) EU reference document good practices on leakage management. Office for Official Publications of the European Communities, Luxembourg

Fecarotta O, Aricò C, Carravetta A, Martino R, Ramos H (2014) Hydropower potential in water distribution networks: pressure control by PATs. Water Resour Manag 29:699. https://doi.org/10.1007/s11269-014-0836-3

Giugni M, Fontana N, Ranucci A (2014) Optimal location of PRVs and turbines in water distribution systems. J Water Resour Plan Manag 140(9):06014004. https://doi.org/10.1061/(ASCE)WR.1943-5452.0000418

Lambert A, Thornton J (2012) Pressure: bursts relationships: Influence of pipe materials, validation of scheme results, and implications of extended asset life. Proc., IWA Int. Specialized Conf. Water Loss 2012, IWA, The Hague, The Netherlands

Lambert A, Fantozzi M, Thornton J (2013) Practical approaches to modelling leakage and pressure management in distribution systems – progress since 2005. CCWI 12th International Conference on Computing and Control for the Water Industry

Muhammetoglu A, Nursen C, Karadirek IE, Muhammetoglu H (2017) Evaluation of performance and environmental benefits of a full-scale pump as turbine system in Antalya water distribution network. Water Supply 18(1):130–141. https://doi.org/10.2166/ws.2017.087

Patelis M, Kanakoudis V, Gonelas K (2017) Combining pressure management and energy recovery benefits in a water distribution system installing PATs. J Water Supply Res Technol AQUA 66(7):520–527. https://doi.org/10.2166/aqua.2017.018

Saldarriaga J, Salcedo CA (2015) Determination of optimal location and settings of pressure reducing valves in water distribution networks for minimizing water losses. 13th CCWI. Procedia Engineering 119:973–983. https://doi.org/10.1016/j.proeng.2015.08.986

Walski T, Bezts W, Posluszny ET, Weir M, Withman B (2006) Modeling leakage reduction through pressure control. Journal American Water Works Association 98(4):147–155. https://doi.org/10.1002/j.1551-8833.2006.tb07642.x